INVITED PAPERS

Transport and sawtooth oscillations from rotational pumping of a magnetized electron plasma*

B. P. Cluggish[†] and C. F. Driscoll
Department of Physics, 0319, University of California at San Diego, La Jolla, California 92093

Definitive measurements have been made of cross-field transport from "rotational pumping" of a magnetized electron column. Rotational pumping is the collisional dissipation of the axial compressions that are caused by $\mathbf{E}\times\mathbf{B}$ rotation of the column through asymmetric confining potentials; it is analogous to the magnetic pumping that damps poloidal rotation in tokamaks. The transport rate is measured over a wide range of plasma parameters, including four orders of magnitude in temperature. A new theory by Crooks and O'Neil shows excellent agreement with the measured rates when the three-dimensional plasma end shapes are numerically calculated using the measured charge density profiles and temperatures. When the plasma displacement is destabilized by a resistive wall and damped by rotational pumping, a complex, nonlinear evolution is observed: a quiescent period is followed by "sawtooth" oscillations of displacement and temperature accompanied by "bursts" of radial transport. This behavior is due to the nonmonotonic temperature dependence of the transport rate. © *1996 American Institute of Physics.* [S1070-664X(96)90405-8]

I. INTRODUCTION

Collisional cross-field transport due to electric or magnetic field asymmetries is important in many neutral and non-neutral plasma confinement devices. In magnetic mirrors, it has long been postulated that particles resonant with field asymmetries enhance radial diffusion,[1] but experimental verification[2] is difficult. In tokamaks, "magnetic pumping" by a spatially varying magnetic field is thought to dissipate poloidal rotation.[3] In non-neutral traps, confinement times much greater than the rotation and transit times are important for a number of technologies and experiments;[4–6] but trap asymmetries can degrade this confinement.[7,8] These plasmas are often approximated as two-dimensional guiding center fluids[9,10] on the rotational time scale, with three-dimensional (3-D) collisions causing dissipative or viscous effects.[11,12]

Here, we present measurements of radial particle transport and resulting mode damping from "rotational pumping" of a magnetized electron column displaced from the axis of a cylindrical trap. Rotational pumping is the collisional dissipation of the axial compressions that are caused by $\mathbf{E}\times\mathbf{B}$ rotation of the column through asymmetric confinement potentials; here, the confinement potentials appear asymmetric only because of the displacement of the column away from the symmetry axis of the trap. We find that this transport conserves particle number; conserves angular momentum by moving the column back to the trap axis as the column expands; and conserves total energy by dissipating electrostatic energy into thermal energy. This dissipation is analogous to that caused by the "second" or "bulk" viscosity[13] in polyatomic gases, which causes weak absorption of sound

waves;[14] here, it causes readily measured particle transport.

The measured transport rate is proportional to the electron–electron collision rate, which drops precipitously in the cryogenic, strongly magnetized regime; surprisingly, the transport is otherwise independent of the magnetic field strength. The observed transport rates are in close agreement with a new theory by Crooks and O'Neil[15] when the 3-D plasma end shapes are numerically calculated using the measured charge density profiles and temperatures. When the plasma displacement is destabilized by a resistive wall and damped by rotational pumping, a complex, nonlinear evolution is observed: a quiescent period is followed by "sawtooth" oscillations of displacement and temperature accompanied by "bursts" of radial transport. This behavior is due to the nonmonotonic temperature dependence of the transport rate; a simple model shows that the system is initially in a stable equilibrium that bifurcates into limit cycles when the plasma radius becomes sufficiently large.

We confine the electron plasmas in a Penning–Malmberg trap,[16,17] shown schematically in Fig. 1. Electrons from a tungsten filament are confined in a series of conducting cylinders of radius $R_w = 1.27$ cm, enclosed in a vacuum can at 4.2 K. The electrons are confined axially by negative voltages $V_c = -200$ V on cylinders 1 and 4; radial confinement is provided by a uniform axial magnetic field, with $10 < B < 60$ kG. The trapped plasma typically has initial density $10^9 \leq n \leq 10^{10}$ cm^{-3}, radius $R_p \sim 0.06$ cm, length $L_p \sim 3$ cm, with a characteristic expansion time $10^2 \leq \tau_m < 10^3$ s. The apparatus is operated in an inject/manipulate/dump cycle, and has a shot-to-shot reproducibility of $\delta n/n \sim 1\%$.

The self-electric field of the electrons cause an $\mathbf{E}\times\mathbf{B}$ drift rotation around an axis through the center of charge, at a rate $500 \leq f_E \leq 3000$ kHz. When the column is displaced from the center of the trap, image charges in the conducting
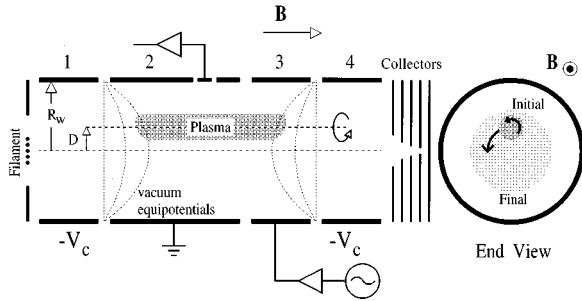

FIG. 1. Schematic of the cylindrical apparatus and electron plasma. End view shows initial and final plasma states.

walls cause the column to orbit around the trap axis in the $m=1$ "diocotron" mode, at frequency $5 \leq f_d \leq 20$ kHz. The image charge signal received on a wall sector is proportional to the displacement, D, of the column from the trap axis.

The z-integrated density of the plasma is measured by dumping the electrons onto the end collectors, by grounding cylinder 4. A rough histogram is obtained from the charge on the five collectors. We obtain a more accurate z-integrated density $q(\rho)=\int dz\, n(\rho,z)$ by using many shots and varying the displacement of the column with each shot. Here, ρ refers to the radius from the plasma axis, i.e., $\mathbf{r}=\mathbf{D}+\boldsymbol{\rho}$. The parallel plasma temperature, $T_\parallel$, is measured by slowly ramping the voltage on cylinder 4 to ground, and measuring the number of electrons that escape as a function of the confining voltage. We can have $0.003 \leq T_\parallel \leq 20$ eV, giving axial electron bounce frequencies $4\times10^5 \leq \omega_b/2\pi \leq 3\times10^7$ Hz, and $T_\parallel$ to $T_\perp$ collisional equilibration rates $10^3 \leq \nu_{\perp\parallel} \leq 10^5$ s^{-1}.

We calculate the 3-D plasma density $n(x,y,z)$ and potential $\phi(x,y,z)$ from the measured $n_z(\rho)$, D, and $T_\parallel$, by numerically solving Poisson's equation on a $125\times125\times200$ grid. Here, we assume

$$n(x,y,z)=n_0(x,y)\exp[e\phi(x,y,z)/kT_\parallel], \qquad (1)$$

where $n_0(x,y)$ follows from $\int dz\, n(x,y,z)=q(\rho)$, where $\rho^2=(x-D)^2+y^2$.

The electrons tend to cool through cyclotron radiation. At $B=40$ kG, the measured radiative cooling time is $\tau_{\mathrm{rad}}=0.29$ s,[16] about 25% longer than predicted by the Larmor formula for an electron in free space. Because $\tau_{\mathrm{rad}}\gg\nu_{\perp\parallel}^{-1}$, the perpendicular and parallel temperatures are presumed to be nearly equal, i.e., $T_\perp \approx T_\parallel \approx T$.

II. CONSERVED QUANTITIES

In this section, we present measurements of a typical 10 s evolution of a plasma during rotational pumping transport. Figure 2 shows the evolution of the plasma displacement D, radius R_p, and temperature T. The plasma column is initially displaced from the trap axis by an amount $D/R_w=0.18$. As the plasma expands radially, D decreases. Here, the "plasma radius" is defined by $R_p \equiv (1.5/N)\int d^3\rho\, \rho n(\rho,z)$. (For a uniform density column, R_p is the radius of the column.) As time goes on, D decreases at a continually faster rate as R_p continues to grow. The temperature, initially $T=0.06$ eV, rapidly increases, but after 0.5 s starts to slowly decrease due to cyclotron radiation. The radiation time τ_{rad} at $B=40$ kG is
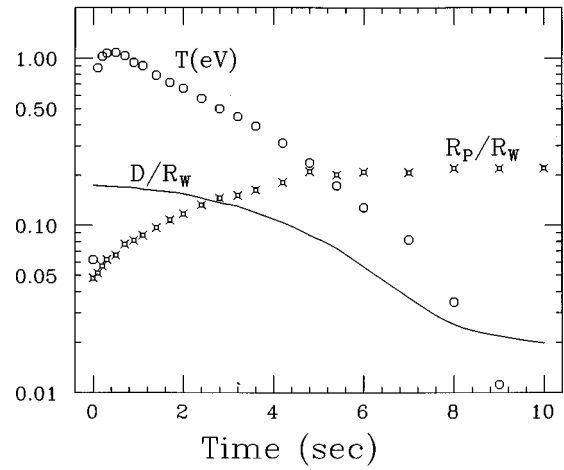

FIG. 2. Rotational pumping causes the plasma radius to increase as the displacement decreases. The initially cold plasma heats up and then slowly cools on a time scale much larger than $\tau_{\mathrm{rad}}=0.29$ s.

much shorter than the time over which T decreases, indicating that the cyclotron cooling is nearly balanced by slowly diminishing Joule heating in the plasma. Finally, D and R_p level off at constant values when T drops below 0.01 eV.

Figure 3 shows the radial density profile at the axial center of the plasma, $n(\rho,z=0)$, at three different times during the evolution: 0, 1.7, and 10 s. The initially narrow, high-density plasma undergoes considerable radial expansion, causing a decrease in the central density by a factor of 8 over the 10 s evolution. Despite the large changes in density profile, the total number of electrons in the plasma, N, is conserved to within 1%. No electrons are lost to the trap walls or over the potential barriers at the end.

The plasma displacement D decreases as the plasma radius R_p increases, with total angular momentum being well conserved. In these highly magnetized plasmas, the total angular momentum is dominated by the electromagnetic component, i.e.

$$P_\theta \equiv \int d^3\mathbf{r}\, n\left(mv_\theta r-\frac{eB}{2c}r^2\right) \approx \frac{eB}{2c}N[D^2+\langle\rho^2\rangle],$$
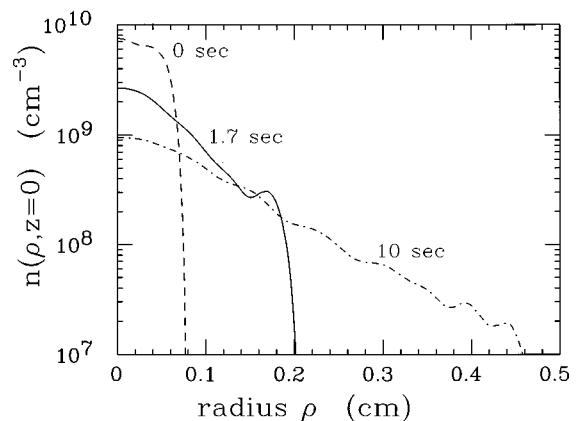

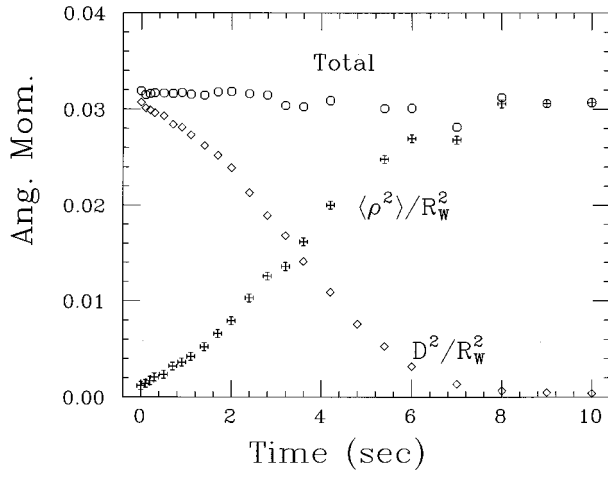FIG. 3. Measured plasma density profiles at three different times as rotational pumping causes plasma expansion.

FIG. 4. The sum of the plasma radius and displacement components of total angular momentum is a constant.

FIG. 5. The sum of the electrostatic, radiated, thermal, and power supply components of the total energy is a constant.

where $\langle \rho^2 \rangle \equiv (1/N) \int d^3\rho \; \rho^2 n(\rho,z)$ is the mean square radius of the plasma. Figure 4 shows the measured values of $\langle (\rho/R_w)^2 \rangle$ and $(D/R_w)^2$ over the 10 s evolution. Initially, 97% of the angular momentum is in $(D/R_w)^2$. As the plasma expands radially, D simultaneously decreases, so that by 10 s only 1% of the angular momentum is in $(D/R_w)^2$. The sum of $\langle (\rho/R_w)^2 \rangle$ and $(D/R_w)^2$ is constant, however, indicating that P_θ is conserved. The forces causing the transport must be azimuthally symmetric about the trap axis.

The expansion/damping process converts the plasma's electrostatic energy, H_ϕ, into thermal energy, H_T. To measure the total energy balance in the plasma, we calculate the energy lost to cyclotron radiation, H_{rad}; as well as the work done by the plasma on the power supplies, W_{ps}, as they maintain the end cylinders at constant voltage. The values of H_ϕ, H_T, H_{rad}, and W_{ps} per electron are calculated as

$$H_\phi = -\frac{1}{2N} \int d^3x \; n(x,y,x) e \phi(x,y,z),$$

$$H_T = \frac{3}{2} kT, \qquad H_{\mathrm{rad}} = \frac{3}{2} \int_0^t \frac{kT}{\tau_{\mathrm{rad}}} \, dt',$$

$$W_{\mathrm{ps}} = -\frac{1}{2} \frac{\Delta Q}{N} V_c,$$

where $\Delta Q(t)$ is the change in the amount of charge on the end cylinders since $t=0$.

Figure 5 shows the evolution of H_ϕ, H_T, W_{ps}, and H_{rad}. Over the 10 s evolution, H_ϕ decreases by 40% from its initial value as the plasma column expands. About 6% of this energy is recovered in W_{ps} because the confining potentials compress the plasma axially as its space charge potential decreases. The electrostatic energy released is converted into heat, increasing H_T over the first 0.5 s, until the Joule heating is balanced by cyclotron cooling. The dissipation of H_ϕ into H_T indicates that $\mathbf{E} \times \mathbf{B}$ drift dynamics alone (which conserve H_ϕ) cannot be responsible for the observed transport. The total energy of the plasma, $H_\phi + W_{\mathrm{ps}} + H_T + H_{\mathrm{rad}}$, remains cons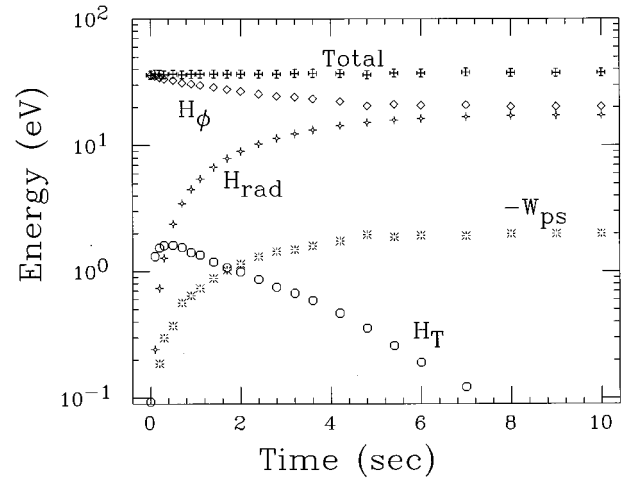tant over the evolution. This indicates that the plasma is not coupled to any unknown energy sources or sinks, and that the forces causing the transport are not time dependent.

III. TRANSPORT RATES

Conservation of P_θ allows us to characterize the transport by the rate of decrease of the displacement of the column, which can be measured nondestructively. (This rate is also the damping rate of the $m=1$ diocotron mode.) The displacement of a constant temperature plasma is observed to decrease exponentially with time, i.e., $D = D_0 \exp(-\gamma t)$, for $D_0 < R_p$. Experimentally, we maintain a constant plasma temperature by applying a 2 MHz oscillation to cylinder 3, thus balancing the radiative cooling. We observe that γ is independent of the frequency and amplitude of the heating oscillation, except through the plasma temperature.

We have measured the damping rate, γ, as a function of several plasma parameters for $D_0 \ll R_p$, and find several unique signatures. One is that, for moderate temperatures, γ
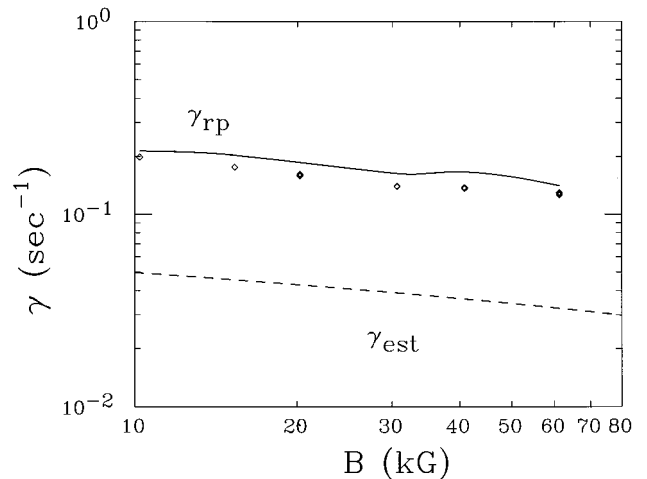

FIG. 6. Measured transport and damping rate γ is nearly independent of the magnetic field for $r_c > b$. Estimated (γ_{est}) and exact (γ_{rp}) theory predictions are shown.
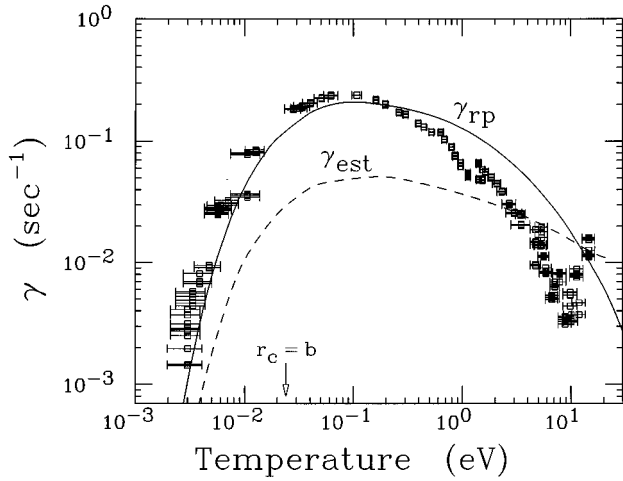
FIG. 7. Measured transport and damping rate γ drops precipitously with decreasing temperature when $r_c < b$.

is nearly independent of magnetic field strength, as shown in Fig. 6. As B is increased from 10 to 60 kG, γ decreases only about 30%. This is counterintuitive, as transport rates usually scale with $\mathbf{E} \times \mathbf{B}$ drift velocities or the mean cyclotron radius, r_c, both of which decrease with B. Indeed, previous experiments on non-neutral plasmas have found transport rates that scaled as B^{-1} (Ref. 11) or B^{-2}.[8,18]

An even more striking signature of the transport is the dependence of γ on temperature, as shown in Fig. 7. The damping rate drops by two orders of magnitude as the temperature is decreased from 0.01 to 0.003 eV. At these temperatures, r_c is smaller than the distance of closest approach, $b \equiv e^2/kT$. In this strongly magnetized regime the temperature equilibration rate, $\nu_{\perp\parallel}$, becomes exponentially small because colliding electrons cannot get close enough together to exchange perpendicular and parallel kinetic energy.[17,19] This is a strong indication that $\gamma \propto \nu_{\perp\parallel}$. The decrease in γ at temperatures above 0.1 eV is also consistent with this dependence, as $\nu_{\perp\parallel} \propto T^{-3/2}$ at high temperatures.

IV. ROTATIONAL PUMPING THEORY

A recent theory of rotational pumping by Crooks and O'Neil[15] proposes that the plasma expands because the potentials produced by the confining voltages on the end cylinders are not azimuthally symmetric about the *plasma* axis, as shown in Fig. 1. Thus, a tube of plasma is alternately compressed and rarefied as it $\mathbf{E} \times \mathbf{B}$ drifts around the plasma axis, producing a modulation in its parallel temperature.

Crooks and O'Neil assume that the Debye length is small, i.e., $\lambda_D \ll L_p$. Thus, the potential along a field line is uniform inside the plasma and abruptly increases at the ends, so that the bounce length of an electron is independent of its energy. The electrons move freely along the field lines, and specularly reflect off the "hard" ends of the plasma. The length of a tube of plasma at radius ρ is then described by

$$L(\rho,t) = L_0(\rho) + \delta L(\rho) \cos \omega_R t, \tag{2}$$

where $\delta L \ll L_0$ and $\omega_R(\rho)/2\pi = f_E(\rho) - f_d$ is the rotation frequency of the plasma in the diocotron mode frame, where the

center of charge of the plasma is stationary. Ignoring radiation, the evolution of $T_\perp$ and $T_\parallel$ in the tube of plasma are described by the equations

$$\frac{d}{dt} T_\perp(\rho,t) = \nu_{\perp\parallel}(\rho)(T_\parallel - T_\perp), \tag{3}$$

$$\frac{d}{dt} T_\parallel(\rho,t) = -2\nu_{\perp\parallel}(\rho)(T_\parallel - T_\perp) - \frac{2}{L} \frac{dL}{dt} T_\parallel. \tag{4}$$

The $-(2/L)(dL/dt)T_\parallel$ term is the rate of increase of internal energy of an ideal gas as it is compressed, i.e., $dW/dt = p\, dV/dt$. We solve these equations perturbatively, as was done by Beck.[16] We assume that to zeroth order in $\delta L/L_0$, $T_\perp^{(0)} = T_\parallel^{(0)} = T(\rho)$, where the superscript denotes the order. To first order, assuming $\nu_{\perp\parallel} \ll \omega_R$,

$$T_\perp^{(1)} = -2T \frac{\delta L}{L_0} \frac{\nu_{\perp\parallel}}{\omega_R} \sin \omega_R t, \tag{5}$$

$$T_\parallel^{(1)} = -2T \frac{\delta L}{L_0} \left(\cos \omega_R t - 2 \frac{\nu_{\perp\parallel}}{\omega_R} \sin \omega_R t \right). \tag{6}$$

The modulation of $T_\parallel^{(1)}$ is nearly in phase with the modulation in L, but a fraction $2\nu_{\perp\parallel}/\omega_R$ of $T_\parallel^{(1)}$ is scattered into $T_\perp^{(1)}$. (Note that $\nu_{\perp\parallel}/\omega_R$ is always less than 1 in a non-neutral plasma.) The second term in Eq. (6), multiplied by dL/dt in Eq. (4), gives an irreversible heating to second order. The rate of change of the thermal energy density in the tube of plasma, averaged over a plasma rotation, is

$$\frac{1}{2} nk \left\langle \frac{d(T_\parallel + 2T_\perp)}{dt} \right\rangle_{\text{rot}} = 2nkT\nu_{\perp\parallel} \left(\frac{\delta L}{L_0} \right)^2, \tag{7}$$

where the brackets denote averaging over a rotation. Crooks and O'Neil assume that $\omega_b \gg \omega_R$, so that the electron bounce action is an adiabatic invariant, and $T_\parallel$ and $T_\perp$ are uniform along the magnetic field. Conservation of energy implies that the rotation-averaged rate of change in thermal energy equals the rotation-averaged Joule heating caused by radial transport, i.e.,

$$\langle -e\Gamma_\rho(\rho)E_\rho(\rho) \rangle_{\text{rot}} = \frac{1}{2} nk \left\langle \frac{d(T_\parallel + 2T_\perp)}{dt} \right\rangle_{\text{rot}}. \tag{8}$$

Using Eq. (7), we obtain an expression for the rotation-averaged, radial electron flux in the frame of an observer located at the center of charge of the plasma column,

$$\Gamma_\rho(\rho) = \frac{2nkT\nu_{\perp\parallel}}{-eE_\rho} \left(\frac{\delta L}{L_0} \right)^2, \tag{9}$$

where $E_\rho(\rho)$ is the radial electric field in the $m=1$ diocotron mode frame.

V. COMPARISON BETWEEN THEORY AND EXPERIMENT

The damping rate of the $m=1$ diocotron mode, γ, can be calculated from the radial flux by using the continuity equation and conservation of angular momentum:
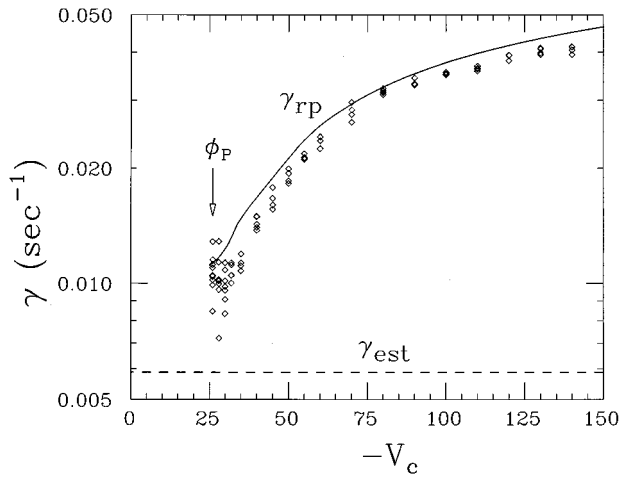
FIG. 8. Measured transport and damping rate γ decreases as V_c approaches the plasma potential ϕ_p.

$$\gamma \equiv -\frac{1}{D}\frac{dD}{dt} = \frac{1}{D^2}\frac{\langle \rho^2 \rangle}{dt}$$

$$\equiv \frac{1}{ND^2}\int 2\pi\rho \, d\rho \, \rho^2 \frac{1}{\rho}\frac{\partial}{\partial\rho}(\rho\Gamma_\rho). \qquad (10)$$

This integral can be solved easily if the plasma is a column of uniform density and temperature with radius R_p and length L_p, and a simple estimate is made of δL.

The length variation δL can be estimated if the plasma ends are assumed to be far from the confining cylinders. In that case, the confining equipotential surfaces near the trap axis are parabolas of revolution described by $z=(j_{01}/4R_w)r^2$, where $j_{01}\approx 2.4$ is the first zero of the J_0 Bessel function. Assuming δL is determined solely by the curvature of these equipotentials gives

$$\delta L = j_{01}(D/R_w)\rho. \qquad (11)$$

Using these approximations, a theoretical estimate of the $m=1$ diocotron mode damping rate is given by

$$\gamma_{\text{est}} = 2j_{01}^2 \nu_{\perp\parallel}\left(\frac{\lambda_D}{L_0}\right)^2 \frac{(R_p/R_w)^2}{1-(R_p/R_w)^2}, \qquad (12)$$

where the factor $1-(R_p/R_w)^2$ appears in the denominator because the $m=1$ diocotron mode is a negative energy mode. Less dissipation of electrostatic energy is required than if the mode energy was positive.

The estimated damping rate γ_{est} is independent of D and depends on B only through the Coulomb logarithm in $\nu_{\perp\parallel}$, in agreement with the experiments. Furthermore, γ_{est} drops off rapidly with decreasing temperature when $r_c < b$ holds, i.e., when the electrons are strongly magnetized. We have plotted γ_{est} in Figs. 6–8 as dashed curves; it is generally a factor of 4 to 6 times lower than the measured γ.

Much closer agreement with the data is obtained by numerically calculating $n(x,y,z)$ and $\phi(x,y,z)$ from the measured $n_z(\rho)$ and $T_\parallel$, using these 3-D density and potential profiles to obtain Γ_ρ, and then numerically integrating Eq. (9). We denote the theoretical rotational pumping damping

rates obtained in this way as γ_{rp}. The γ_{rp} are plotted in Figs. 6–8 as solid curves and are in much closer agreement with the data than the γ_{est}. The primary reason for this discrepancy is that Eq. (11) is often not a good approximation to the plasma end shape, as discussed in the next section.

The discrepancy between the data and the solid curve in Fig. 7 at temperatures above 0.2 eV may be because at high enough temperatures $\lambda_D \sim \delta L$, so the ends of the plasma can no longer be considered "hard." Thus, the length of a tube of plasma is no longer well described by Eq. (2). The discrepancy may also be a systematic error. If the plasma temperature increases with ρ, the damping rate will be smaller than the measured value of $T_\parallel$ at the plasma center would indicate for $r_c > b$.

In addition to D, B, and T, we have measured the dependence of γ on n, R_p, and L_p. In all cases, we find agreement between γ_{rp} and experiment comparable to the agreement in Figs. 6–8. Crooks and O'Neil also predict that when $\omega_b < \omega_R$, the transport may be greatly enhanced by electrons whose bounce and rotation frequencies are resonant. We do not observe any enhancement, but these resonances should not exist in our experiments, since $\omega_b \approx \nu_{\perp\parallel}$ when $\omega_b < \omega_R$.

VI. END SHAPES OF OFF-AXIS PLASMAS

The central idea of the Crooks and O'Neil theory is that the transport depends on an asymmetry in the shape of the plasma ends. We have found that the plasma end shape depends on V_c, R_p, and T. Figure 8 shows the dependence of the measured damping rate on the confinement voltage V_c. As V_c approaches the plasma potential ϕ_p, the ends of the plasma get closer to the "flat" equipotential surfaces at the boundaries between the end cylinders and the grounded cylinders, as shown in Fig. 1. This decreases δL, thus decreasing γ and providing a direct test of the theory of Crooks and O'Neil. The γ_{est} curve in Fig. 8 is independent of V_c because Eq. (12) assumes the plasma ends are far from the confining cylinders, i.e., $V_c \gg \phi_p$.

It is evident from Fig. 8 that even when V_c is large enough that the plasma is well confined, γ is still larger than γ_{est}. The reason for this is that space charge fields tend to increase δL beyond the estimate in Eq. (11). We have investigated this effect by numerically calculating 3-D density profiles from test data with uniform temperature and uniform z-integrated density. The simulated plasmas have $\phi_p \ll V_c$, with $n \sim 10^7$ cm^{-3} and $L_p/R_w \approx 7$. As in Ref. 20, we define an "end slant" coefficient C_s by

$$C_s = \frac{1}{2}\frac{R_w}{D}\left(\frac{\partial}{\partial\rho}\delta L\right)_{\rho=0}, \qquad (13)$$

where the factor of $\frac{1}{2}$ takes into account the two ends of the plasma.

Figure 9 shows C_s as a function of R_p/R_w at four different temperatures. The solid line is an analytical estimate of C_s for a zero-temperature plasma by Peurrung and Fajans.[20] This estimate includes the effect of the curvature of the confining and image charge equipotentials, but not the space charge equipotentials. At large R_p/R_w, the numerical C_s agree fairly well with the analytical estimate; but as R_p/R_w
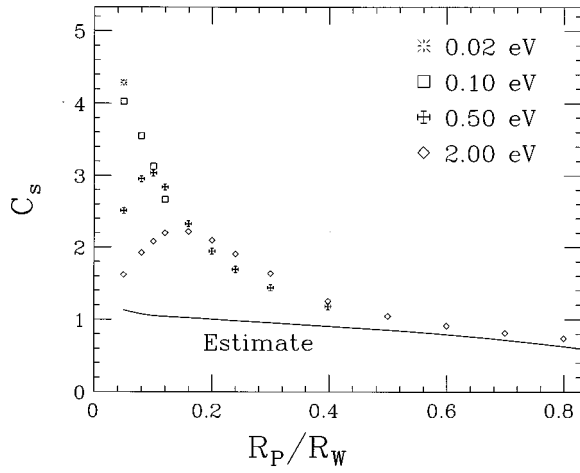
FIG. 9. Numerical calculation of the "end slant" coefficient versus the plasma radius at four different temperatures. The analytical estimate is from Ref. 20; the divergence from the estimate at small R_p is due to space-charge effects.

decreases, C_s increases much faster than the estimate. For $R_p \gg \lambda_D$, C_s is independent of temperature, but as R_p approaches λ_D, C_s tends to decrease with temperature. This indicates that the anomalous increase in C_s is due to the space-charge electric fields.

The increase in C_s at small R_p explains why γ_{rp} is generally four to six times larger than γ_{est} in Figs. 6–8; this data was measured on plasmas with $R_p/R_w \sim 0.1$. Similarly, the decrease in C_s with T at small R_p/R_w explains the difference in slope between γ_{rp} and γ_{est} in Fig. 7 at temperatures above 1 eV.

VII. SAWTOOTH OSCILLATIONS

When the $m=1$ diocotron mode is destabilized by a resistive wall, a complex, nonlinear evolution of D is observed, as shown in Fig. 10. The initial, linear growth of D due to the resistive wall saturates after 20 s, and is followed by a quiescent period during which D is stable. At $t \simeq 110$ s,
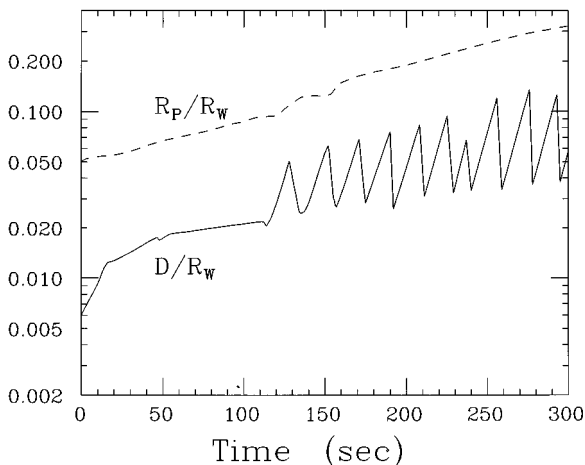
the diocotron mode destabilizes again, and D undergoes "sawtooth" oscillations that can last for thousands of seconds.

A simple model shows that this complicated "dance" of the diocotron mode is caused by the nonmonotonic temperature dependence of the temperature equilibration rate $\nu_{\perp\parallel}$. For any given plasma there exists an equilibrium temperature T_{eq} and displacement D_{eq} where Joule heating balances cyclotron cooling, and the resistive growth of D is balanced by rotational pumping damping. In Fig. 10, this equilibrium is initially stable because $\partial \nu_{\perp\parallel}/\partial T < 0$ at $T = T_{eq}$ (i.e., $r_c > b$), giving rise to the quiescent period from $t = 20$ to $t = 100$ s. However, the slow increase in R_p due to the rotational pumping transport causes T_{eq} to slowly decrease until eventually $\partial \nu_{\perp\parallel}/\partial T > 0$ at $T = T_{eq}$ (i.e., $r_c < b$). The onset of sawtooth oscillations in D is thus a Hopf bifurcation into limit cycles around an unstable equilibrium. Numerical integration of the evolution equations shows that each decrease in D is accompanied by a temperature "spike" and a burst of radial transport. The amplitude of the oscillations is strongly dependent on the minimum plasma temperature set by background transport.

VIII. CONCLUSIONS

From a fluid perspective, rotational pumping can be thought of as dissipation of a compressible flow by a second viscosity ζ, where the dissipation rate is $\gamma \propto \zeta (\nabla \cdot \mathbf{v})^2$. In the guiding center approximation, the cyclotron motion of the electrons is a "hidden" degree of freedom, like the vibrations and rotations of gas molecules.[14] Equilibration of hidden and translational degrees of freedom gives rise to a second viscosity.[13] The second viscosity coefficient in these plasmas can be expressed as

$$\zeta = \frac{4}{9} \frac{nT}{\nu_{\perp\parallel}} \frac{1}{1 + (\omega_R/3\nu_{\perp\parallel})^2}. \tag{14}$$

In our experiments, γ is independent of ω_R because $\omega_R \gg \nu_{\perp\parallel}$ and $(\nabla \cdot \mathbf{v})^2 \propto \omega_R^2$.

This rotational pumping mechanism should also damp diocotron modes with $m \geq 2$. It may also cause the dissipation of several otherwise stable non-neutral plasma configurations, including two electron vortex equilibria,[21] vortex crystals,[22] asymmetric equilibria,[10] and toroidal electron plasmas.[23] Rotational pumping is analogous to magnetic pumping, which is presumed to strongly damp poloidal rotation in tokamaks.[3] Similarly, rotational pumping should strongly damp azimuthal rotation in nonaxisymmetric systems, such as tandem mirrors.[1,2]

FIG. 10. Typical evolution of plasma displacement and radius when the diocotron mode is destabilized by a resistive wall.

[1] D. D. Ryutov and G. V. Stupakov, Fiz. Plazmy **4**, 521 (1978).

[2] D. L. Goodman, C. C. Patty, and R. S. Post, Phys. Fluids B **2**, 2173 (1990); E. B. Hooper, Jr., R. H. Cohen, D. L. Correll, J. M. Gilmore, and D. P. Grubb, Phys. Fluids **28**, 3609 (1985); H. D. Price, A. J. Lichtenberg, M. A. Lieberman, and M. Tuszewski, Nucl. Fusion **23**, 1043 (1983).

[3] T. H. Stix, Phys. Fluids **16**, 1260 (1973); W. M. Stacey and D. R. Jackson, Phys. Fluids B **5**, 1828 (1993).

[4] L. H. Haarsma, K. Abdullah, and G. Gabrielse, Phys. Rev. Lett. **75**, 806 (1995).

[5] J. J. Bollinger, D. J. Wineland, and J. H. Dubin, Phys. Plasmas **1**, 1403 (1994).

[6] R. W. Gould and M. A. LaPointe, Phys. Rev. Lett. **67**, 3685 (1991).

[7] D. L. Eggleston and J. H. Malmberg, Phys. Rev. Lett. **59**, 1675 (1987).

[8] C. F. Driscoll, K. S. Fine, and J. H. Malmberg, Phys. Fluids **29**, 2015 (1986).

[9] X.-P. Huang and C. F. Driscoll, Phys. Rev. Lett. **72**, 2187 (1994); T. B. Mitchell and C. F. Driscoll, Phys. Rev. Lett. **73**, 2196 (1994).

[10] J. Notte, A. J. Peurrung, and J. Fajans, Phys. Rev. Lett. **69**, 3056 (1992); J. Notte and J. Fajans, Phys. Plasmas **1**, 1123 (1994).

[11] C. F. Driscoll, J. H. Malmberg, and K. S. Fine, Phys. Rev. Lett. **60**, 1290 (1988).

[12] T. M. O'Neil, C. F. Driscoll and D. H. E. Dubin, in *Turbulence and Anomalous Transport in Magnetized Plasmas*, edited by D. Gresillon (Editions de Physique, Orsay, 1987), pp. 293–308.

[13] L. D. Landau and E. M. Lifshitz, *Fluid Mechanics*, 2nd ed. (Pergamon, Oxford, 1987), Sec. 81.

[14] J. D. Lambert, *Vibrational and Rotational Relaxation in Gases* (Clarendon, Oxford, 1977), Sec. 2.2.

[15] S. M. Crooks and T. M. O'Neil, Phys. Plasmas **2**, 355 (1995).

[16] B. R. Beck, Ph.D. dissertation, University of California, San Diego, 1990.

[17] B. R. Beck, J. Fajans, and J. H. Malmberg, Phys. Rev. Lett. **68**, 317 (1992).

[18] C. F. Driscoll and J. H. Malmberg, Phys. Rev. Lett. **50**, 167 (1983).

[19] M. E. Glinsky, T. M. O'Neil, M. N. Rosenbluth, K. Tsuruta, and S. Ichimaru, Phys. Fluids B **4**, 2720 (1992).

[20] A. J. Peurrung and J. Fajans, Phys. Fluids B **5**, 4250 (1993).

[21] T. B. Mitchell, C. F. Driscoll, and K. S. Fine, Phys. Rev. Lett. **71**, 1371 (1993).

[22] K. S. Fine, A. C. Cass, W. G. Flynn, and C. F. Driscoll, Phys. Rev. Lett. **75**, 3277 (1995).

[23] S. S. Khirwadkar, P. I. John, K. Avinash, A. K. Agarwal, and P. K. Kaw, Phys. Rev. Lett. **71**, 3443 (1993).